

SUPPLEMENTAL EXPERIMENTAL PROCEDURES

Adoptive transfer, detection and characterization of antigen-specific CD8⁺ T cells.

Peripheral blood leukocytes (PBLs) containing 500 WT or *Tcf7*^{-/-} OT-I T cells (Thy1.2⁺CD45.2⁺) were adoptively transferred into B6.SJL recipient mice (Thy1.2⁺CD45.1⁺) alone, or in the presence of Thy1.1⁺CD45.2⁺ WT OT-I reference T cells at 1:1 ratio. Twenty-four hours later, the recipient mice were infected with either attenuated LM-Ova or VacV-Ova as described previously (Badovinac and Harty, 2007). On various days post-infection, PBLs or splenocytes were isolated from the recipient mice, and donor-derived antigen-specific T cells were identified by surface staining of differential Thy1 and CD45 genetic markers. For additional phenotypic analysis, the cells were surface-stained for KLRG1 (clone 2F1), IL-7R α (clone A7R34), CD62L (clone MEL-14, BD Biosciences), and IL-2R β (clone TM- β 1, BD Biosciences). CCR7 was stained indirectly with purified CCL19-Fc fusion protein followed by anti-human Fc γ according to manufacturer's instructions (eBioscience). For detection of IL-15 α chain, splenocytes were first blocked with rat serum, goat serum, and free streptavidin (1 μ g/ml), and stained with biotinylated IL-15R α (R&D Systems) or control goat IgG, followed by incubation with fluorochrome-conjugated streptavidin (McGill et al. 2010). For functional characterization of antigen-specific CD8⁺ T cells, splenocytes were stimulated with 200 nM of Ova₂₅₇₋₂₆₄ peptide (SIINFEKL) for 5-6 hrs in the presence of GolgiStop and GlogiPlug (BD Biosciences). The stimulated cells were then surfaced stained, fixed and permeabilized using BD Cytofix/Cytoperm and BD Perm/Wash solutions (BD Biosciences), and intracellularly stained for IFN- γ (clone XMG1.2), IL-2

(clone JES6-5H4), TNF- α (clone TN3-19), and Granzyme B (clone GB11, Invitrogen) following standard protocols (Haring et al., 2008). Bcl-2 was detected by intracellular staining with Bcl-2 PE set (clone 3F11, BD Biosciences). For intranuclear staining of transcription factors, surface-stained cells were fixed and permeabilized using Foxp3 staining buffer set (eBioscience), and stained with either PE-conjugated T-bet (clone 4B10, Santa Cruz Biotechnology) or Eomes antibody (clone Dan11mag, eBioscience). All fluorochrome-conjugated antibodies were from eBioscience unless indicated otherwise. The stained cells were analyzed on a FACSCalibur flow cytometer followed by data analysis using FlowJo software (Tree Star, Inc)(Jing et al., 2008).

Detection of BrdU uptake and activated Caspase-3 and -7 in antigen-specific CD8⁺ T cells

To determine the proliferation rate of antigen-specific T cells at early contraction phase, the mice were *i.p.* injected with 1 mg of 5-bromo-2-deoxyuridine (BrdU) on day 7 post-infection with *actA*LM-OVA and given 0.8 mg/ml BrdU in drinking water for additional 18 hours. Splenocytes were isolated, surface-stained to identify donor-derived OT-I cells, followed by fixation and permeabilization procedures as recommended in the BrdU Flow Kit (BD Biosciences). For detection of activated caspase-3 and -7 in antigen-specific T cells, splenocytes were surface-stained as above and then incubated with the fluorescent inhibitor of caspases reagent at 37°C for 60 min as recommended in the Vybrant FAM Caspase-3 and -7 assay kit (Invitrogen).

***In vitro* proliferation of memory CD8⁺ T cells in response to IL-15**

Splenocytes were isolated from B6.SJL recipients of WT or *Tcf7*^{-/-} OT-I T cells on day 90 after LM-Ova infection. The cells were labeled with 2.5 μM CFSE as described (Jabbari and Harty, 2006), and 1×10⁶ cells were cultured in 12-well plate in the presence or absence of 50 ng/ml (Peptrotech). IL-15 was refreshed at the end of 3-day culture. CFSE dilution on CD8⁺CD45.2⁺ memory T cells was tracked daily during days 2-5 of culture. The total splenocytes were used to facilitate transpresentation of IL-15 to T cells (Dubois et al., 2002).

***In vivo* cytolytic assay**

Splenocytes from C57BL/6 mice (CD45.2⁺) were labeled with 0.2 μM or 2 μM CFSE. The CFSE^{low} cells were pulsed with 1 μM OVA₂₅₇₋₂₆₄ peptide, mixed with unpulsed CFSE^{high} cells at 1:1 ratio, and a total number of 8 × 10⁶ mixed cells were injected into immune or naïve B6.SJL (CD45.1⁺) mice with the naïve mice as no-killing controls (Barber et al., 2003; Pham et al., 2009). Four hours later, spleens were harvested, and killing target cells were identified by CD45.2 positivity, within which the percentages of CFSE^{low} and CFSE^{high} cells were determined by flow cytometry. The specific killing was calculated using the following formula:

$$\left(1 - \frac{\frac{\text{Percent of CFSE}^{\text{low}} \text{ in immune mice}}{\text{Percent of CFSE}^{\text{high}} \text{ in immune mice}}}{\frac{\text{Percent of CFSE}^{\text{low}} \text{ in naïve mice}}{\text{Percent of CFSE}^{\text{high}} \text{ in naïve mice}}} \right) \times 100\%$$

Detection of memory CD8⁺ T cells in tissues

Isolation of lymphocytes from the livers and lungs was performed essentially as described (Masopust et al., 2001). Mice were first anesthetized, perfused with Hanks' balanced salt solution (HBSS), and then lungs and livers were removed. Lung tissue was minced and treated with Collagenase D (125 units/ml, Roche Applied Science) and DNase I (6 units/ml, Roche Applied Science). Liver tissue was mashed through a 70- μ m strainer in HBSS and subjected to gradient centrifugation using Percoll. Cells at the gradient interface were harvested, washed, and surface-stained for CD8, CD45, and Thy1 markers to identify donor-derived memory CD8⁺ T cells. Lymph nodes and bone marrow cells were harvested as previously described (Xue et al., 2007) and stained similarly.

Retroviral transduction

Bicistronic retroviral vector MigR1 and that expressing WT Eomes were obtained from Dr. Steven Reiner (Intlekofer et al., 2007). Retroviruses were packaged by transient transfection of 293T cells with the retroviral vector along with pCL^{eco} as described (Xue et al., 2002). Retroviral transduction of antigen-specific CD8⁺ T cells was performed following a previously described procedure (Joshi et al., 2007). In brief, WT or *Tcf7*^{-/-} OT-I TCR transgenic mice were infected with 2.5×10^7 CFU attenuated LM-Ova, and one day later the splenocytes were harvested and spin-infected with control or Eomes-expressing retrovirus in the presence of 8 μ g/ml polybrene and 100 units/ml IL-2, followed by 30 min incubation at 37 degrees. The retrovirally infected cells were transferred into B6.SJL recipients (0.2×10^6 cells/mouse), and 24 hours later the

recipients were infected with 5×10^6 CFU attenuated LM-Ova. Expansion and memory formation of antigen-specific CD8⁺ T cells were monitored in PBLs on various days post-infection.

Microarray and bioinformatics analysis

On days 70-80 post-infection of B6.SJL recipient mice that had received 500 WT or *Tcf7*^{-/-} OT-I T cells, splenocytes were harvested and surface-stained to identify CD45.2⁺CD8⁺V α -2⁺ cells. These donor-derived memory CD8⁺ T cells were sorted directly into Trizol LS reagent (Invitrogen). After chloroform extraction, the aqueous phase was mixed with 2 volumes of ethanol and loaded onto a purification column in RNeasy Mini Kit (Qiagen) for further purification. RNA quality was assessed using the Agilent Model 2100 Bioanalyzer. Total RNAs from 3 WT and 3 *Tcf7*^{-/-} memory CD8⁺ T cells (500 pg) were amplified using the NuGEN WT-Ovation Pico RNA Amplification System (NuGEN). The resulting cDNA probes were hybridized to the GeneChip Mouse GENE 1.0 ST arrays (Affymetrix), scanned with the Affymetrix Model 7G upgraded scanner, and the data were collected using the GeneChip Operating Software (GCOS). The data were imported into Partek Genomics Suite using RMA (Robust Multi-Chip Average) normalization. Differential expression and its statistical significance were calculated using linear contrasts with an ANOVA (analysis of variance) model. Functional annotation of these genes were performed using DAVID bioinformatics resources (<http://david.abcc.ncifcrf.gov>) (Huang da et al., 2009).

Wnt responsiveness of naïve and memory CD8⁺ T cells

Naïve OT-I CD8 T cells were purified by negative selection, and day 60-100 memory CD8⁺ T cells were isolated by cell sorting. The cells were treated with DMSO, BIO-acetoxime or N-methylated BIO (each at 5 µM) for 12 hours in 24-well plate. For responsiveness of CD8⁺ T cells to a Wnt ligand, Wnt3a conditioned medium was used. L cells expressing Wnt3a or control L cells were cultured in complete DMEM containing 10% FBS. Exponentially growing cells were re-plated, and 6 days later the Wnt3a conditioned medium or control medium was collected and used for stimulation of CD8⁺ T cells. The stimulated cells were then harvested, and gene expression was determined using quantitative PCR.

Quantitative RT-PCR

Total RNA was reverse-transcribed using QuantiTech Reverse Transcription Kit (Qiagen). The resulting cDNA was analyzed for expression of different genes by quantitative PCR using SYBR Advantage qPCR pre-mix (Clontech) on ABI 7300 Real Time PCR System (Applied Biosystems). Relative gene expression levels in each sample were normalized to that of a housekeeping gene, hypoxanthine phosphoribosyltransferase 1 (*Hprt1*). For each individual gene, its relative expression in DMSO-treated cells was arbitrarily set to 1, and its expression changes in BIO-acetoxime- or N-methylated BIO-treated cells were calculated as fold repression or induction.

Design of PCR primers was assisted by using the Primer3 program (Rozen and Skaletsky, 2000). The primers used in quantitative RT-PCR were as follows:

Eomes: 5'-TCCTAACACTGGCTCCCACT and 5'-GTCACCTCCACGATGTGCAG;

Myc: 5'-GTACCTCGTCCGATTCCACG and 5'-GCCTCTTCTCCACAGACACC;
Tbx21: 5'-CAATGTGACCCAGATGATCG and 5'-GCGTTCTGGTAGGCAGTCAC; *Tcf7*: 5'-
CAATCTGCTCATGCCCTACC and 5'-CTTGCTTCTGGCTGATGTCC;
Hprt1: 5'-GCGTCGTGATTAGCGATGATG and 5'-CTCGAGCAAGTCTTTCAGTCC; *Axin2*:
5'-AAGAGAAGCGACCCAGTCAA and 5'-CTGCGATGCATCTCTCTCTG.

For assessing enrichment of genomic DNA segment in ChIP, the following primers were used.

Axin2 T2/3 cluster: 5'-AAATCCACAGCGCAGTTTTT and 5'-TTCAACCCAGGTCCTGTTTC;

Axin2 T7/8 cluster: 5'-TGTGTGGAGCTCAGATTTTCG and 5'-
ATGTGAGCCTCCTCTCTGGA;

Rag2 promoter: 5'-CACTCTACCCTGCAGCCTTC and 5'-TCTGCCCTCTTG TAGCCAGT;

Tbx21 5'-regulatory region: 5'-GTGCCATGGTGCATGTTT TAG and 5'-
GGGTGGTGGTTTGTCTGACT;

For the *Eomes* allele, -10 kb: 5'-CCCAGCGGGATGTTAATACT and 5'-
ACCCGGATCTCACTGTAGGA;

-3.5 kb (cluster a): 5'-AGAGAACAAAGGGCCAAACA and 5'-
ACTTTGCCTGGACTCTGGAA;

-2.6 kb (element b): 5'-CATGGAAGGTCCTGCTGTTT and 5'-
TCTGGTGTCTCAGGCACACT;

-1.8 kb (element c): 5'-CCTTGTGGAATCCTCACGTT and 5'-
CAGTCCAGAGATCCCAGCTC;

-0.8 kb (element d): 5'-CAGCTGCTAGGGAACCTTTG and 5'-
AATCCCTCTGCTCGGTTTT; and

+3 kb: 5'-TCCTAACACTGGCTCCCACT and 5'-CACAGGCTTTTCCAGTCTCC.

Experimental Procedure-Associated References

Badovinac, V.P., and Harty, J.T. (2007). Manipulating the rate of memory CD8⁺ T cell generation after acute infection. *J Immunol* *179*, 53-63.

Barber, D.L., Wherry, E.J., and Ahmed, R. (2003). Cutting edge: rapid in vivo killing by memory CD8 T cells. *J Immunol* *171*, 27-31.

Dubois, S., Mariner, J., Waldmann, T.A., and Tagaya, Y. (2002). IL-15Ralpha recycles and presents IL-15 In trans to neighboring cells. *Immunity* *17*, 537-547.

Haring, J.S., Jing, X., Bollenbacher-Reilly, J., Xue, H.H., Leonard, W.J., and Harty, J.T. (2008). Constitutive expression of IL-7 receptor alpha does not support increased expansion or prevent contraction of antigen-specific CD4 or CD8 T cells following *Listeria monocytogenes* infection. *J Immunol* *180*, 2855-2862.

Huang da, W., Sherman, B.T., and Lempicki, R.A. (2009). Systematic and integrative analysis of large gene lists using DAVID bioinformatics resources. *Nature protocols* *4*, 44-57.

Intlekofer, A.M., Takemoto, N., Kao, C., Banerjee, A., Schambach, F., Northrop, J.K., Shen, H., Wherry, E.J., and Reiner, S.L. (2007). Requirement for T-bet in the aberrant differentiation of unhelped memory CD8⁺ T cells. *J Exp Med* *204*, 2015-2021.

Jabbari, A., and Harty, J.T. (2006). Secondary memory CD8⁺ T cells are more protective but slower to acquire a central-memory phenotype. *J Exp Med* *203*, 919-932.

Jing, X., Zhao, D.M., Waldschmidt, T.J., and Xue, H.H. (2008). GABPbeta2 is dispensible for normal lymphocyte development but moderately affects B cell responses. *The Journal of biological chemistry* *283*, 24326-24333.

Joshi, N.S., Cui, W., Chandele, A., Lee, H.K., Urso, D.R., Hagman, J., Gapin, L., and Kaech, S.M. (2007). Inflammation directs memory precursor and short-lived effector CD8⁽⁺⁾ T cell fates via the graded expression of T-bet transcription factor. *Immunity* *27*, 281-295.

Masopust, D., Vezys, V., Marzo, A.L., and Lefrancois, L. (2001). Preferential localization of effector memory cells in nonlymphoid tissue. *Science* *291*, 2413-2417.

McGill, J., Van Rooijen, N., and Legge, K.L. (2010) IL-15 trans-presentation by pulmonary dendritic cells promotes effector CD8 T cell survival during influenza virus infection. *J Exp Med.* *207*, 521-534.

Pham, N.L., Badovinac, V.P., and Harty, J.T. (2009). A default pathway of memory CD8 T cell differentiation after dendritic cell immunization is deflected by encounter

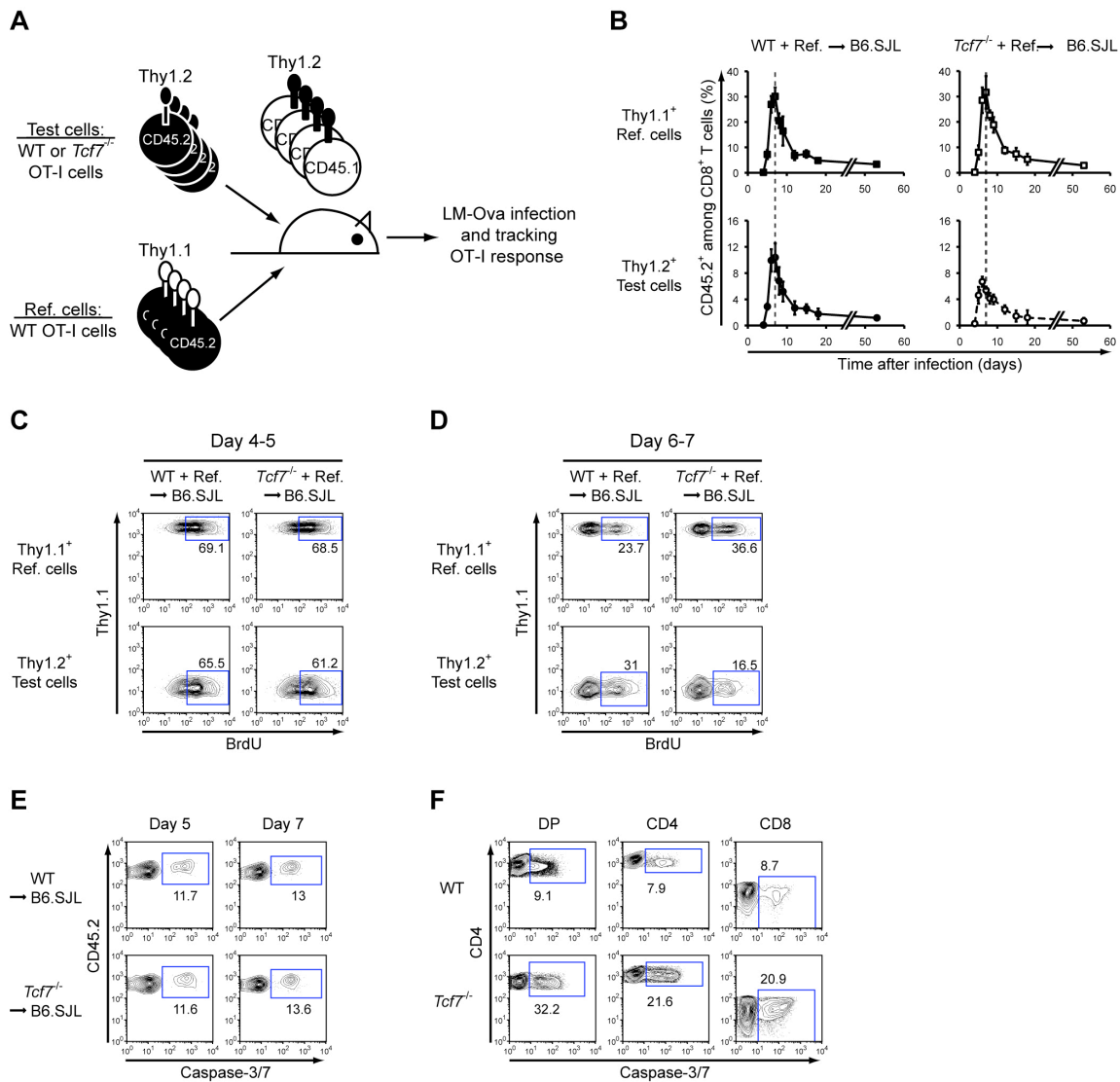
with inflammatory cytokines during antigen-driven proliferation. *J Immunol* 183, 2337-2348.

Rozen, S., and Skaletsky, H. (2000). Primer3 on the WWW for general users and for biologist programmers. *Methods Mol Biol* 132, 365-386.

Xue, H.H., Bollenbacher-Reilley, J., Wu, Z., Spolski, R., Jing, X., Zhang, Y.C., McCoy, J.P., and Leonard, W.J. (2007). The transcription factor GABP is a critical regulator of B lymphocyte development. *Immunity* 26, 421-431.

Xue, H.H., Fink, D.W., Jr., Zhang, X., Qin, J., Turck, C.W., and Leonard, W.J. (2002). Serine phosphorylation of Stat5 proteins in lymphocytes stimulated with IL-2. *Int Immunol* 14, 1263-1271.

Zhou et al. Supplemental Figure 1



Supplemental Figure 1 (related to Figure 1). TCF-1 deficiency limited expansion but did not affect survival of effector CD8⁺ T cells.

(A) Schematic showing the experimental design for (B) - (D). Five hundreds of WT or *Tcf7*^{-/-} OT-I CD8⁺ T cells (expressing CD45.2 and Thy1.2, as test cells) were mixed with CD45.2⁺Thy1.1⁺ OT-I CD8⁺ T cells (as reference cells, ref. cells) at approximately 1:1 ratio, and transferred into CD45.1⁺ B6.SJL recipients, which were *i.v.* infected with 5×10^6 CFU of *actA*⁻LM-Ova. Donor-derived antigen-specific CD8⁺ T cells were identified by CD45.2 positivity, and the sources of test and reference cells were distinguished by differential Thy1.2 and Thy1.1 expression.

(B) Kinetics of CD8⁺ T cell response after LM infection. OT-I CD8⁺ T cells were tracked in the PBLs on different days post-infection, and their percentages in CD8 T cells are shown. Data are representative from 2 independent experiments with 5 recipient mice examined in each experiment.

(C) and (D) Proliferation of antigen-specific CD8⁺ T cells during expansion phase. LM-infected recipients were *i.p.* injected with 1 mg of BrdU on day 4 (C) or day 6 (D) after

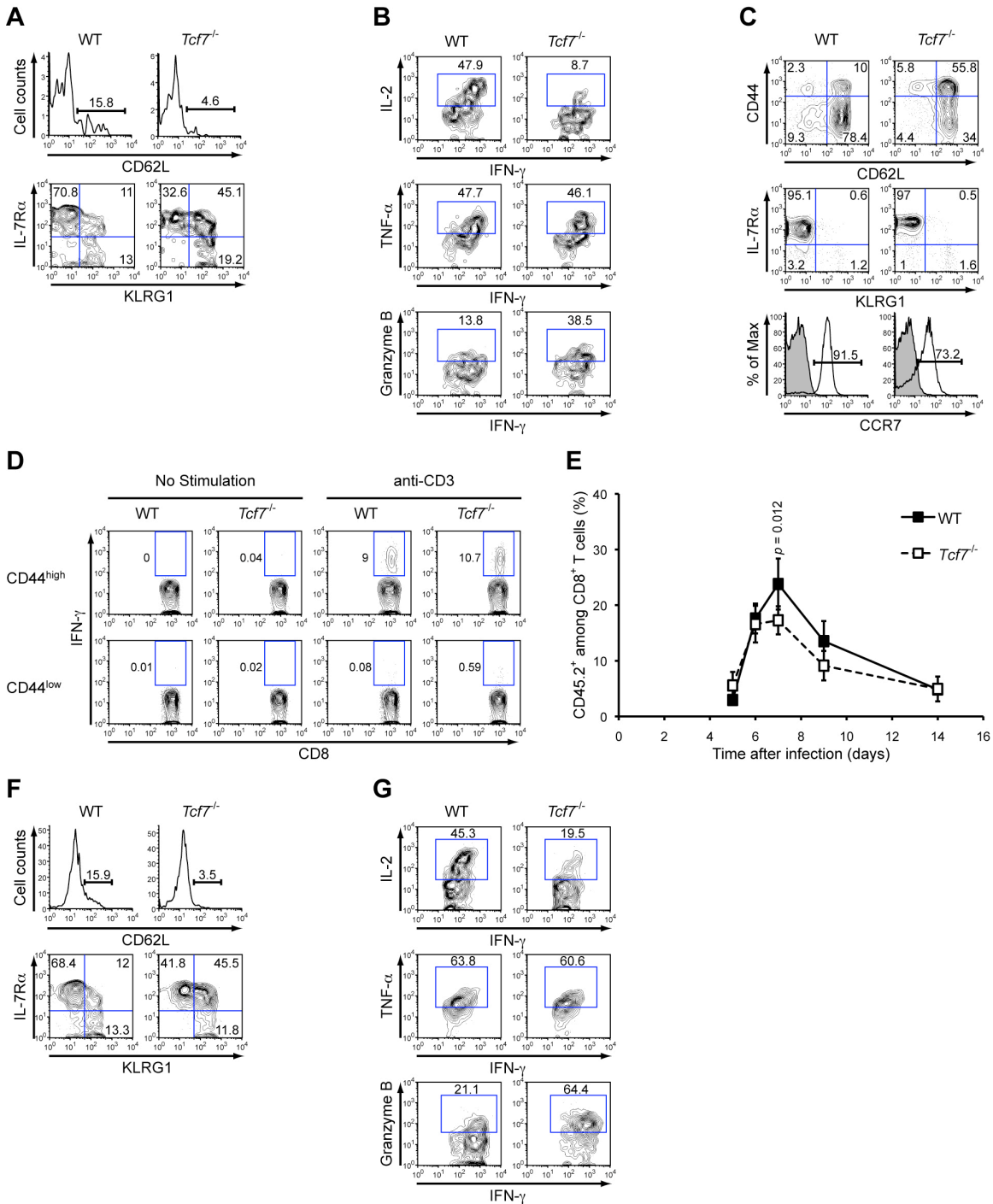
infection, and 18 hrs later, BrdU uptake by OT-I T cells were measured. Data are representative from 2 independent experiments with similar results.

(E) Apoptosis of effector CD8⁺ T cells. In separate experiments where WT or *Tcf7*^{-/-} OT-I T cells were transferred into B6.SJL recipients without Thy1.1⁺ reference cells, on days 5 or 7 after infection, activation status of caspase-3/7 was determined in effector OT-I T cells.

Percentages of cells with active caspase-3/7 are shown.

(F) *Tcf7*^{-/-} thymocytes showed increased caspase-3/7 activity. Thymocytes were isolated from WT or *Tcf7*^{-/-} mice, surface stained for CD4 and CD8, and then stained for active caspase-3/7. Percentages of caspase-3/7-positive subsets were shown for DP, CD4⁺, and CD8⁺ thymocytes. Data are representative of analysis of 3 pairs of WT and *Tcf7*^{-/-} mice. This finding is consistent with previous observations that TCF-1-dependent signals are required for thymocyte survival (Ioannidis et al., Nat. Immunol. 2, 691-697, 2001).

Zhou et al. Supplemental Figure 2



Supplemental Figure 2 (related to Figure 2). Impaired Tcm differentiation of $Tcf7^{-/-}$ memory CD8⁺ T cells generated in response to viral infection or from naïve precursors. (A) and (B) B6.SJL recipients of WT or $Tcf7^{-/-}$ OT-I CD8⁺ T cells were infected with 4×10^6 PFU of vaccinia virus expressing Ova (VacV-Ova). At days 45-75 post-infection, memory OT-I cells were characterized by cell surface or intracellular staining. (A) CD62L, IL-7R α , and KLRG1 expression on memory OT-I cells. Percentage of each subset was shown. (B) Production of IL-2, TNF- α , and granzyme B by memory OT-I cells. Splenocytes were

stimulated with Ova-peptide for 6 hrs and intracellularly stained for the indicated effector molecules. Gating of the positive population was based on respective positive control.

(C) Phenotypic analysis of splenic *Tcf7*^{-/-} OT-I T cells before adoptive transfer. Splenocytes were isolated from WT or *Tcf7*^{-/-} OT-I TCR transgenic mice and surfaced stained. Percentage of each subset was shown. Data are representative of at least 3 independent experiments with similar results.

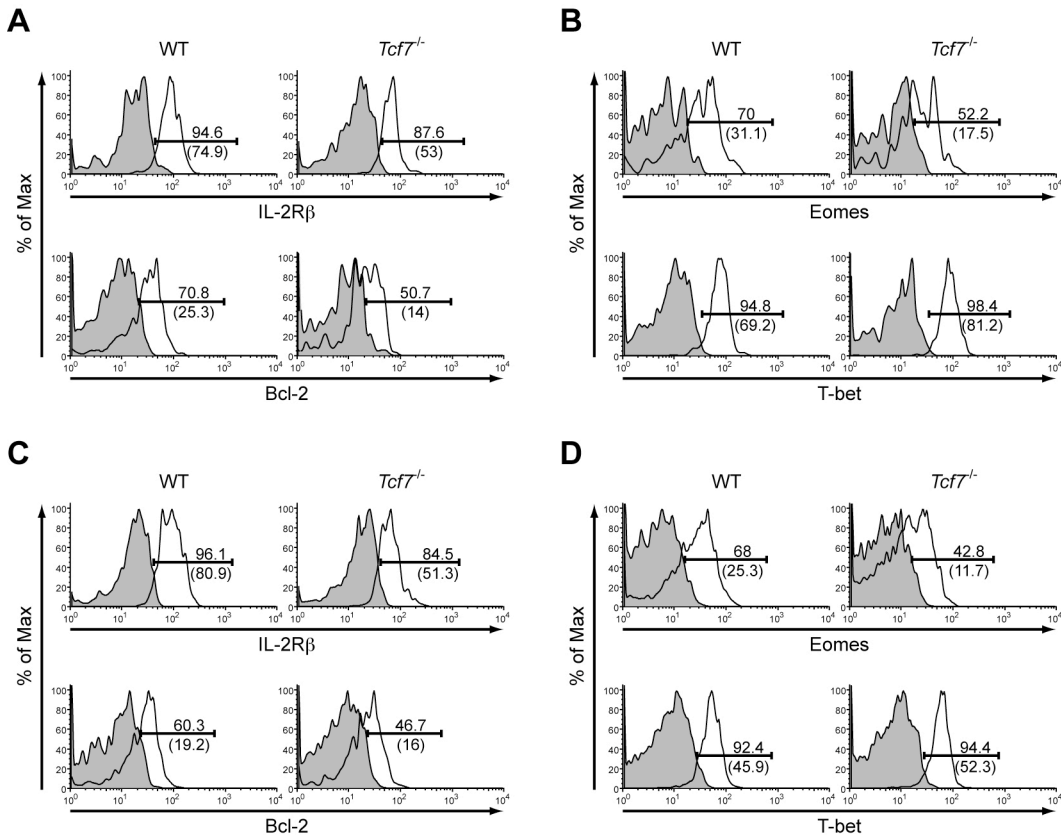
(D) Functional analysis of splenic *Tcf7*^{-/-} CD8⁺ T cells before adoptive transfer. CD44^{hi} and CD44^{lo} OT-I T cells were either cultured without stimulation or stimulated with plate-bound anti-CD3 (1 µg/ml) for 5 hrs. Brefeldin A was included for the last 4 hrs of incubation. The cells were then intracellularly stained for IFN-γ and the percentages of IFN-γ⁺ subsets are shown. Neither WT nor *Tcf7*^{-/-} CD44^{lo} CD8⁺ T cells constitutively expressed or were induced to express granzyme B or IL-2 (data not shown).

(E) Kinetics of early CD8⁺ T cell responses using naïve precursors. Naïve CD62L⁺CD44^{lo} CD8⁺ T cells were isolated from the spleens of WT or *Tcf7*^{-/-} OT-I TCR transgenic mice by cell sorting. Five hundreds of the sorted naïve precursors were adoptively transferred into B6.SJL recipients followed by infection with attenuated LM-Ova. Expansion and contraction of effector OT-I T cells were tracked in PBLs. Data are representative of 2 independent experiments with similar results (n = 5 for each time point).

(F) and (G) Characterization of memory OT-I cells derived from naïve precursors. During days 39-46 post-infection, memory OT-I cells were characterized by cell surface or intracellular staining. (F) CD62L, IL-7Rα, and KLRG1 expression on memory OT-I cells. Percentage of each subset was shown. (G) Production of IL-2, TNF-α, and granzyme B by memory OT-I cells. Splenocytes were stimulated with Ova-peptide for 6 hrs and intracellularly stained for the indicated effector molecules. Gating of the positive population was based on respective isotype control.

Note that the reduced production of IL-2 by *Tcf7*^{-/-} memory CD8⁺ T cells may not have direct functional consequence on memory CD8⁺ differentiation, as indicated by several recent studies showing that paracrine IL-2 signaling rather than intrinsic IL-2 production impacts primary and secondary CD8⁺ T cell responses (Williams et al., Nature 441, 890-893, 2006; Kalia et al., Immunity 32, 91-103, 2010; Pipkin et al., Immunity 32, 79-90, 2010).

Zhou et al. Supplemental Figure 3



Supplemental Figure 3 (related to Figure 3). Diminished expression of IL-2Rβ, Bcl-2, and Eomes in *Tcf7*^{-/-} memory CD8⁺ T cells generated in response to viral infection or from naïve precursors.

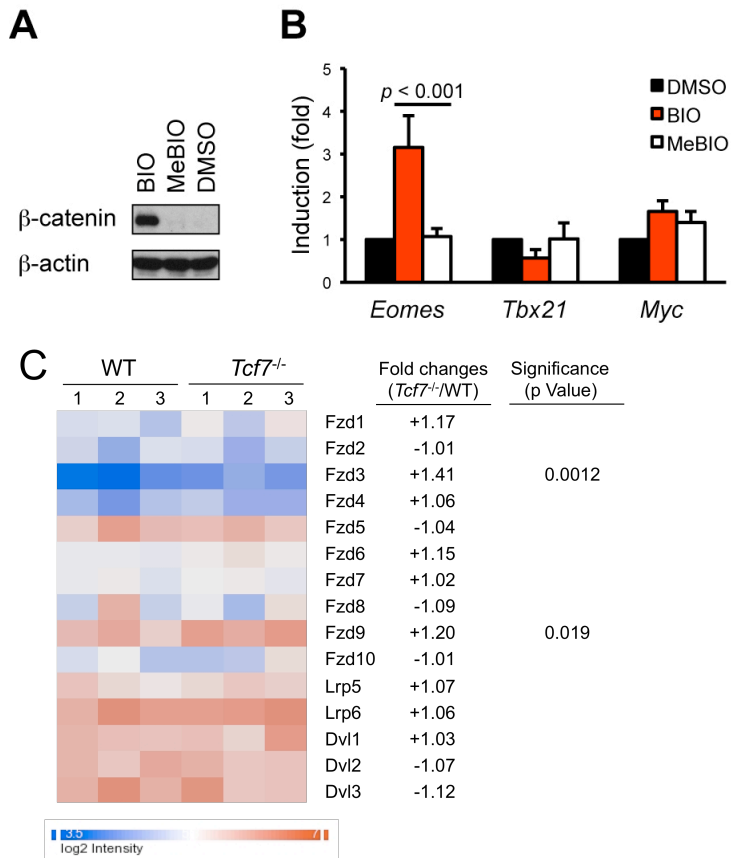
(A) and (B) B6.SJL recipients of WT or *Tcf7*^{-/-} OT-I CD8⁺ T cells were infected with VacV-Ova as in Figure S2A, and memory OT-I cells were characterized by cell surface or intracellular staining during days 45-75 after infection.

(C) and (D) WT or *Tcf7*^{-/-} naïve CD62L⁺CD44^{lo} OT-I T cells were sorted and transferred into B6.SJL recipients, followed by LM-Ova infection as in Figure S2E. Memory OT-I cells were analyzed during 39-46 days after infection.

(A) and (C) Expression of IL-2Rβ and Bcl-2 in memory OT-I cells.

(B) and (D) Eomes and T-bet expression in memory OT-I cells. Percentage of each positive subset was shown. Also shown in the parenthesis is the ΔMFI value between antibody- and isotype-stained whole cell populations without positivity gating as in Figure 3C. All data are representative of 2 independent experiments.

Zhou et al. Supplemental Figure 4



Supplemental Figure 4 (related to Figure 5). Wnt responsiveness of CD8⁺ T cells.

(A) BIO-acetoxime but not MeBIO induced β -catenin accumulation in naïve CD8⁺ T cells. Naïve CD8 T cells were isolated from WT OT-I TCR transgenic mice and stimulated as indicated for 12 hrs. β -catenin and β -actin were detected by Western blotting.

(B) Induction of *Eomes* by BIO-acetoxime. Naïve CD8 T cells were isolated and stimulated for 12 hrs as in (A). The expression of selected genes was quantitatively determined, and all normalized to the samples treated with DMSO.

(C) Expression of Fzd receptor complex components in WT and *Tcf7*^{-/-} memory CD8⁺ T cells. The expression data of Fzd receptor complex components were extracted from microarray analysis of WT and *Tcf7*^{-/-} memory CD8⁺ T cells and shown in an intensity map. The color-coded relative expression scale is shown at the bottom. Also shown are expression changes between *Tcf7*^{-/-} and WT memory CD8⁺ T cells, with “+” denoting induction and “-” denoting repression. The p value of gene expression changes is shown for those reached statistical significance.

Zhou et al. Supplemental Figure 5

Cluster a

-3527

Mouse ggaacacagggcagaagtagcagatctggccatcagagaa**caaag**ggccaaacagtgaacctgag
Rat ggaacacagggctgaggtagtagatctggccatcagagaa**caaag**gggcgaacagtgaacctgag
Human gaaagcacagcagaggtggcagatctggccatcagagaa**caaag**ggccaaagagtgaacctgag
Chimp gaaagcacagcagaggtggcagatctggccatcagagaa**caaag**ggccaaagagtgaacctgag
Dog caaagcgcagtgagggtggcaggtctggccagcagagaa**caaag**ggccaaagagttaacctgag

-3477

Mouse atggtgaaataaaatgtaacatca**caaag**agagggccatagataaaatagtaaaaggaccaact
Rat acgctgaaataaaatgtaacatca**caaag**agagggccatagataaaataggaaaaggaccaact
Human ttggtgaaataaaatgtaacatca**caaag**aaagggccatagataaaatagtaaaaggaccaact
Chimp atggtgaaataaaatgtaacatca**caaag**aaagggccatagataaaatagtaaaaggaccaact
Dog atggtgaaataaaatgtaacatca**caaag**aaagggccatagataaaatagttaaaggaccaact

-3318

Mouse ttttcctaggggttaaaggagagcatgcagcaagcctgttcagaattta**caaag**tgtttgaata
Rat ttttcctaggggttaaaggagagcatgcagcaagcctgttcagaattta**caaag**tgtttgaata
Human ttttcctaggggttaaaggagaaccggcagcaagcctgttcagaattta**caaag**tgtttgaata
Chimp ttttcctaggggttaaaggagaaccggcagcaagcctgttcagaattta**caaag**tgtttgaata
Dog ttttcctaggggttaaaggagaaccggcagcaagcctgttcagaattta**caaag**tgtttgaata

Element b

-2563

Mouse tacaggaggtgctgctgacatgt-----gccctgc**ctttg**ttttctcttcttacttctgg
Rat taagtgagg-gctgctggcccg-----gc-----ttctctttctct
Human taaggaggggtgctgctgacatgttcaacttaagccactg**ctttg**ctttcttttctattctac
Chimp taaggaggggtgctgctgacatgttcaacttaagccactg**ctttg**ctttcttttctattctac
Dog ttaggaggggtgctgctgacatgttcaactgaagccactg**ctttg**ctttcttttctgttctac

Element c

-1815

Mouse cactgtgccacgc-cagcgtttccccgggtctctt-**caaag**tattttgaagggac-----
Rat cactgtgccatgc-cagtgttccccgggtctctt-**caaag**tattttgaagggac-----
Human ca**ctttg**ccacgcgaagcgttccctggctgctgctcaaaagcattttgaagggacgccgagg
Chimp ca**ctttg**ccacgcgaagcgttccctggctgctgctcaaaagcattttgaagggacgccgagg
Dog ca**ctttg**ccacgcgcagcgttccctggccgcctcgaaagcagctctgaagggacaccgaag

Mouse cttact-tctggctgtggt
Rat cctact-tctgactctggt
Human cccgct-tcttg**ctttg**tt
Chimp cccgct-tcttg**ctttg**tt
Dog cccgctttctctctgtgat

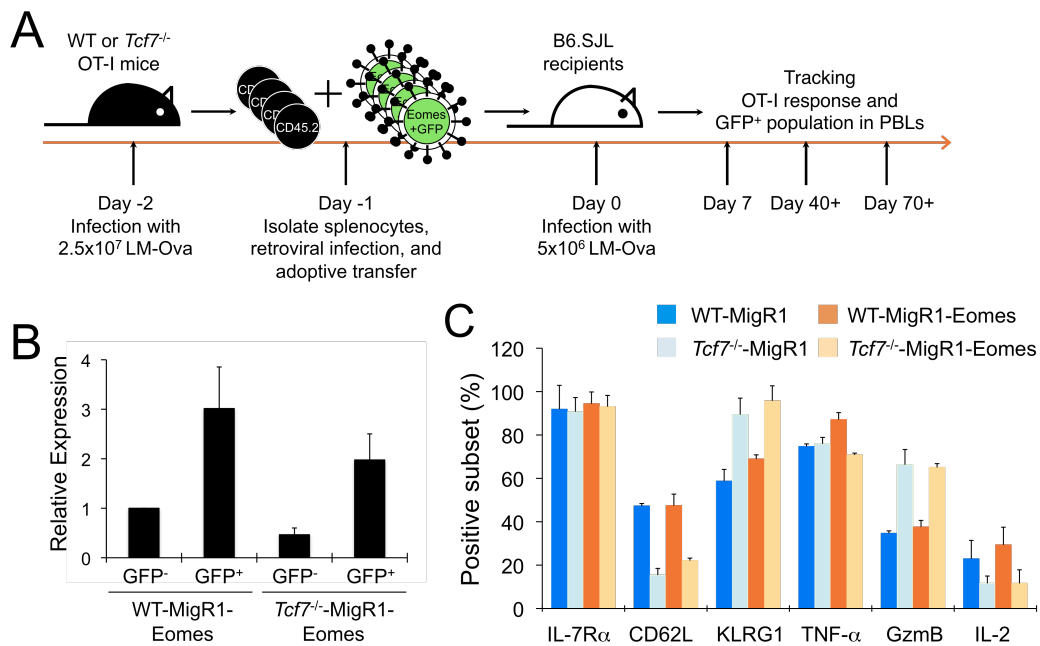
Element d

-837

Mouse cagggaaatcttaactgcacagctgctagggaa**ctttg**tgcttagtgctcagtcaccaccaaag
Rat cagggaaatcttaactgcacagctgctagggaa**ctttg**tgcttagtgctcagtcaccaccaaag
Human cagggaaatcttaactgtggggctgtagggaa**ctttg**ttcttggtgctcagtcaccaccaaag
Chimp cagggaaatcttaactgtggggctgtagggaa**ctttg**ttcttggtgctcagtcaccaccaaag
Dog cagggaaatctcaaccgactgctgctgggaa**ctttg**tctcttggtgccagggccagctgaag

Supplemental Figure 5 (related to Figure 6). Cross-species comparison of the conserved consensus TCF-1 binding motifs in the *Eomes* 5'-regulatory region. The conserved sequences are highlighted and their relative locations marked (based on UCSC genome browser).

Zhou et al. Supplemental Figure 6



Supplemental Figure 6 (related to Figure 7). Effect of forced expression Eomes on WT and *Tcf7*^{-/-} memory CD8⁺ T cells.

(A) Experimental design. WT and *Tcf7*^{-/-} OT-I mice were infected with high dose of LM-Ova, and 24 hours later the splenocytes were harvested, retrovirally transduced, and then transferred into naïve B6.SJL mice. The recipients were then infected with LM-Ova, the percentage of GFP⁺ OT-I in PBL CD8⁺ cells were determined on various days after infection. (B) Validation of increased Eomes expression in GFP⁺ WT or *Tcf7*^{-/-} memory OT-I cells infected with MigR1-Eomes. On day 40 after LM infection, splenocytes were isolated from recipients of WT or *Tcf7*^{-/-} OT-I T cells that had been infected with MigR1-Eomes. GFP⁻ and GFP⁺ CD45.2⁺CD8⁺ cells were separated by cell sorting, and the relative levels of Eomes transcripts were determined by quantitative RT-PCR. (C) Phenotypic and functional analyses of retrovirally transduced WT or *Tcf7*^{-/-} memory T cells. On day 40 after infection, splenocytes were isolated from recipients of retrovirally infected WT or *Tcf7*^{-/-} OT-I T cells. The cells were surface or intracellularly stained after 5-hr Ova peptide stimulation. For surface staining, the percentages of subsets positive for IL-7Rα, CD62L, or KLRG1 in GFP⁺CD45.2⁺CD8⁺ T cells are shown. For intracellular staining, the percentages of subsets positive for TNF-α, Granzyme B (GzmB), or IL-2 in IFN-γ⁺GFP⁺CD45.2⁺CD8⁺ T cells are shown. Note that *Tcf7*^{-/-} memory T cells reproducibly manifested phenotypes as shown in Figure 2, and forced expression of Eomes did not substantially improve/aggravate those phenotypic or functional alterations. Additionally, the numbers of GFP⁺ *Tcf7*^{-/-} memory OT-I cells expressing Eomes in the spleen showed an approximately 1.6-fold increase compared with those of GFP⁺ *Tcf7*^{-/-} memory OT-I cells infected with MigR1 ($1.08 \pm 0.32 \times 10^5$ vs. $0.69 \pm 0.31 \times 10^5$, n=3). The increase, however, did not reach a statistical significance, likely due to variations in retroviral infection efficiency and varied responses to LM infection when different recipients were cross-compared.

Additionally, the numbers of GFP⁺ *Tcf7*^{-/-} memory OT-I cells expressing Eomes in the spleen showed an approximately 1.6-fold increase compared with those of GFP⁺ *Tcf7*^{-/-} memory OT-I cells infected with MigR1 ($1.08 \pm 0.32 \times 10^5$ vs. $0.69 \pm 0.31 \times 10^5$, n=3). The increase, however, did not reach a statistical significance, likely due to variations in retroviral infection efficiency and varied responses to LM infection when different recipients were cross-compared.

**Supplemental Table I. Select Genes Significantly Differentially Expressed
between WT and TCF-1-deficient memory CD8⁺ T cells
(related to Figure 4)**

Fold changes (<i>Tcf7</i> ^{-/-} /WT)	Gene Symbol	Gene Name
Transcription factors		
-1.52	<i>Aebp2</i>	AE BINDING PROTEIN 2
-1.58	<i>Atm</i>	ATAXIA TELANGIECTASIA MUTATED HOMOLOG (HUMAN)
-1.53	<i>Churc1</i>	CHURCHILL DOMAIN CONTAINING 1
-1.53	<i>Ciao1</i>	WD REPEAT DOMAIN 39
-2.55	<i>Eomes</i>	EOMESODERMIN HOMOLOG (XENOPUS LAEVIS)
-1.81	<i>Gtf2b</i>	GENERAL TRANSCRIPTION FACTOR IIB
-1.79	<i>Gtf2i</i>	GENERAL TRANSCRIPTION FACTOR II I
-1.50	<i>Hivep2</i>	HUMAN IMMUNODEFICIENCY VIRUS TYPE I ENHANCER BINDING PROTEIN 2
-1.65	<i>Khdrbs1</i>	KH DOMAIN CONTAINING, RNA BINDING, SIGNAL TRANSDUCTION ASSOCIATED 1
-1.53	<i>Men1</i>	MULTIPLE ENDOCRINE NEOPLASIA 1
-1.50	<i>Mkl2</i>	MKL/MYOCARDIN-LIKE 2
-1.67	<i>Mtf2</i>	METAL RESPONSE ELEMENT BINDING TRANSCRIPTION FACTOR 2
-2.6	<i>Myc</i>	MYELOCYTOMATOSIS ONCOGENE
-1.77	<i>Nab1</i>	NGFI-A BINDING PROTEIN 1
-2.45	<i>Nfib</i>	NUCLEAR FACTOR I/B
-1.72	<i>Nrbf2</i>	NUCLEAR RECEPTOR BINDING FACTOR 2 PSEUDOGENE
-2.14	<i>Pa2g4</i>	PROLIFERATION-ASSOCIATED 2G4
-1.63	<i>Pdlim1</i>	PDZ AND LIM DOMAIN 1 (ELFIN)
-1.85	<i>Purb</i>	PURINE RICH ELEMENT BINDING PROTEIN B
-1.68	<i>Taf10</i>	TAF10 RNA POLYMERASE II, TATA BOX BINDING PROTEIN (TBP)-ASSOCIATED FACTOR
-1.67	<i>Taf11</i>	TAF11 RNA POLYMERASE II, TATA BOX BINDING PROTEIN (TBP)-ASSOCIATED FACTOR
-1.75	<i>Tfam</i>	TRANSCRIPTION FACTOR A, MITOCHONDRIAL
-1.57	<i>Tsg101</i>	TUMOR SUSCEPTIBILITY GENE 101
-1.65	<i>Ubf</i>	UPSTREAM BINDING TRANSCRIPTION FACTOR, RNA POLYMERASE I
-1.53	<i>Ugp2</i>	UDP-GLUCOSE PYROPHOSPHORYLASE 2
-1.67	<i>Yy1</i>	YY1 TRANSCRIPTION FACTOR
-1.64	<i>Zeb1</i>	ZINC FINGER HOMEBOX 1A
1.62	<i>Egr1</i>	EARLY GROWTH RESPONSE 1
1.60	<i>Foxc1</i>	FORKHEAD BOX C1
2.79	<i>Foxd2</i>	FORKHEAD BOX D2
1.56	<i>Foxf1a</i>	FORKHEAD BOX F1A
1.61	<i>Homez</i>	HOMEODOMAIN LEUCINE ZIPPER-ENCODING GENE
1.60	<i>Hoxb2</i>	HOMEO BOX B2
1.54	<i>Insm2</i>	INSULINOMA-ASSOCIATED 2
2.39	<i>Jund</i>	JUN PROTO-ONCOGENE RELATED GENE D1
1.53	<i>Ldb2</i>	LIM DOMAIN BINDING 2
1.61	<i>Lhx9</i>	LIM HOMEODOMAIN PROTEIN 9
1.64	<i>Msx2</i>	HOMEO BOX, MSH-LIKE 2
1.50	<i>Nhlh2</i>	NESSCIENT HELIX LOOP HELIX 2
1.56	<i>Nkx2-3</i>	NK2 TRANSCRIPTION FACTOR RELATED, LOCUS 3 (DROSOPHILA)
1.61	<i>Npas3</i>	NEURONAL PAS DOMAIN PROTEIN 3
1.66	<i>Rhox4b</i>	REPRODUCTIVE HOMEODOMAIN 4B
1.61	<i>Rhox4e</i>	RIKEN CDNA 5430432L21 GENE
1.59	<i>Rhox9</i>	RIKEN CDNA 1600026O01 GENE
1.79	<i>Rybp</i>	RING1 AND YY1 BINDING PROTEIN
1.98	<i>Six6</i>	SINE OCULIS-RELATED HOMEODOMAIN 6 HOMOLOG (DROSOPHILA)
1.54	<i>Smad6</i>	MAD HOMOLOG 6 (DROSOPHILA)
1.52	<i>Sox7</i>	SRF-BOX CONTAINING GENE 7
1.62	<i>Sp3</i>	TRANS-ACTING TRANSCRIPTION FACTOR 3
1.55	<i>Spib</i>	SPI-B TRANSCRIPTION FACTOR (SPI-1/PU.1 RELATED)
1.51	<i>Tbpl2</i>	TBP-RELATED FACTOR 3
1.54	<i>Yap1</i>	YES-ASSOCIATED PROTEIN 1
1.70	<i>Zeb2</i>	ZINC FINGER HOMEODOMAIN 1B
1.53	<i>Zfp213</i>	ZINC FINGER PROTEIN 213
1.55	<i>Zfp354a</i>	ZINC FINGER PROTEIN 354A
1.59	<i>Zfy1</i>	ZINC FINGER PROTEIN 1, Y LINKED
1.54	<i>Zscan2</i>	ZINC FINGER AND SCAN DOMAIN CONTAINING 2
Effector molecules		
6.34	<i>Gzma</i>	GRANZYME A
4.58	<i>Gzmb</i>	GRANZYME B
Cytokines, chemokines, and secreted factors		
-1.64	<i>Clefi</i>	CARDIOTROPIN-LIKE CYTOKINE FACTOR 1
-1.83	<i>Ltb</i>	LYMPHOTOXIN B
-1.95	<i>Mif</i>	MACROPHAGE MIGRATION INHIBITORY FACTOR
-1.51	<i>Spre2</i>	SPROUTY-RELATED, EVH1 DOMAIN CONTAINING 2
-1.89	<i>Tnfrsf8</i>	TUMOR NECROSIS FACTOR (LIGAND) SUPERFAMILY, MEMBER 8
-1.61	<i>Xcl1</i>	CHEMOKINE (C MOTIF) LIGAND 1
1.57	<i>Gdf9</i>	GROWTH DIFFERENTIATION FACTOR 9
1.53	<i>Ifna11</i>	INTERFERON ALPHA FAMILY, GENE 11
1.58	<i>Ntf3</i>	NEUROTROPHIN 3

1.55	<i>Pdgfc</i>	PLATELET-DERIVED GROWTH FACTOR, C POLYPEPTIDE
1.53	<i>Scgb3a1</i>	SECRETOGLOBIN, FAMILY 3A, MEMBER 1
1.67	<i>Shh</i>	SONIC HEDGEHOG
1.54	<i>Tgfa</i>	TRANSFORMING GROWTH FACTOR ALPHA
1.72	<i>Wnt2b</i>	WINGLESS RELATED MMTV INTEGRATION SITE 2B
Cytokine and chemokine receptors		
-1.51	<i>Ccr7</i>	CHEMOKINE (C-C MOTIF) RECEPTOR 7
-1.78	<i>Ccr9</i>	CHEMOKINE (C-C MOTIF) RECEPTOR 9
-1.69	<i>Cxcr3</i>	CHEMOKINE (C-X-C MOTIF) RECEPTOR 3
-1.54	<i>Ifnar2</i>	INTERFERON (ALPHA AND BETA) RECEPTOR 2
-1.69	<i>Il10ra</i>	INTERLEUKIN 10 RECEPTOR, ALPHA
2.31	<i>Cx3cr1</i>	CHEMOKINE (C-X3-C) RECEPTOR 1
2.52	<i>Il12rb2</i>	INTERLEUKIN 12 RECEPTOR, BETA 2
Costimulatory and inhibitor receptors, and adhesion molecules		
-1.53	<i>Cd28</i>	CD28 ANTIGEN
-1.65	<i>Cd5</i>	CD5 ANTIGEN
-2.81	<i>Sell</i>	L-SELECTIN/CD62L
-2.82	<i>Tlr1</i>	TOLL-LIKE RECEPTOR 1
1.76	<i>Itga1</i>	INTEGRIN ALPHA 1
1.72	<i>Itgad</i>	INTEGRIN, ALPHA D
1.65	<i>Itgam</i>	INTEGRIN ALPHA M
1.5	<i>Itgb6</i>	INTEGRIN BETA 6
2.88	<i>Klrp1</i>	KILLER CELL LECTIN-LIKE RECEPTOR SUBFAMILY G, MEMBER 1
Cell cycle regulation		
-1.60	<i>Cdc5</i>	COILED-COIL DOMAIN CONTAINING 5
-1.70	<i>Cdk6</i>	CYCLIN-DEPENDENT KINASE 6
-1.60	<i>Cks1b</i>	CDC28 PROTEIN KINASE 1B
-1.53	<i>Ctef</i>	CCCTC-BINDING FACTOR
-1.56	<i>Dmtf1</i>	CYCLIN D BINDING MYB-LIKE TRANSCRIPTION FACTOR 1
-1.86	<i>Eef1e1</i>	EUKARYOTIC TRANSLATION ELONGATION FACTOR 1 EPSILON 1
-1.52	<i>Gmn</i>	GEMININ
-2.29	<i>Gnl3</i>	GUANINE NUCLEOTIDE BINDING PROTEIN-LIKE 3 (NUCLEOLAR)
-1.69	<i>Gspt1</i>	G1 TO S PHASE TRANSITION 1
-1.60	<i>Htatip2</i>	HIV-1 TAT INTERACTIVE PROTEIN 2, HOMOLOG (HUMAN)
-2.53	<i>Lzts1</i>	LEUCINE ZIPPER, PUTATIVE TUMOR SUPPRESSOR 1
-1.60	<i>Mcm6</i>	MINICHROMOSOME MAINTENANCE DEFICIENT 6 (MIS5 HOMOLOG, S. POMBE)
-1.77	<i>Mnat1</i>	MENAGE A TROIS 1
-1.67	<i>Mns1</i>	MEIOSIS-SPECIFIC NUCLEAR STRUCTURAL PROTEIN 1
-1.72	<i>Npm1</i>	NUCLEOPHOSMIN 1
-1.74	<i>Prdm9</i>	VPR DOMAIN CONTAINING 9
-1.52	<i>Rad50</i>	RAD50 HOMOLOG (S. CERVISIAE)
-1.60	<i>Rassf2</i>	RAS ASSOCIATION (RALGDS/AF-6) DOMAIN FAMILY 2
-1.65	<i>Sesn3</i>	SESTRIN 3
-1.65	<i>Smc4</i>	SMC4 STRUCTURAL MAINTENANCE OF CHROMOSOMES 4-LIKE 1 (YEAST)
-1.55	<i>Spindl</i>	SPINDLIN
-2.02	<i>Terf2</i>	TELOMERIC REPEAT BINDING FACTOR 2
1.52	<i>Cablest1</i>	CDK5 AND ABL ENZYME SUBSTRATE 1
1.55	<i>Dab2ip</i>	DISABLED HOMOLOG 2 (DROSOPHILA) INTERACTING PROTEIN
1.68	<i>Gadd45b</i>	GROWTH ARREST AND DNA-DAMAGE-INDUCIBLE 45 BETA
1.74	<i>Gas1</i>	GROWTH ARREST SPECIFIC 1
1.64	<i>Gas2</i>	GROWTH ARREST SPECIFIC 2
1.77	<i>Yes1</i>	YAMAGUCHI SARCOMA VIRAL (V-YES) ONCOGENE HOMOLOG 1
Apoptosis regulation		
-1.90	<i>Bcap29</i>	B-CELL RECEPTOR-ASSOCIATED PROTEIN 29
-1.51	<i>Bcap31</i>	B-CELL RECEPTOR-ASSOCIATED PROTEIN 31
-1.69	<i>Birc3</i>	BACULOVIRAL IAP REPEAT-CONTAINING 3
-2.16	<i>Casp1</i>	CASPASE 1
-1.64	<i>Clefi</i>	CARDIOTROPHIN-LIKE CYTOKINE FACTOR 1
-1.84	<i>Clec2d</i>	C-TYPE LECTIN DOMAIN FAMILY 2, MEMBER D
-2.43	<i>Cyes</i>	CYTOCHROME C, SOMATIC
-1.53	<i>Fis1</i>	FISSION 1 (MITOCHONDRIAL OUTER MEMBRANE) HOMOLOG (YEAST)
-1.66	<i>Itgb3bp</i>	INTEGRIN BETA 3 BINDING PROTEIN (BETA3-ENDONEXIN)
-1.69	<i>Mlh1</i>	MUTL HOMOLOG 1 (E. COLI)
-1.63	<i>Msh6</i>	MUTS HOMOLOG 6 (E. COLI)
-1.85	<i>Prdx2</i>	PEROXIREDOXIN 2
-1.69	<i>Rnf130</i>	RING FINGER PROTEIN 130
1.58	<i>Acvr1c</i>	ACTIVIN A RECEPTOR, TYPE IC
1.51	<i>Alox12</i>	ARACHIDONATE 12-LIPOXYGENASE
1.68	<i>Bag2</i>	BCL2-ASSOCIATED ATHANOGENE 2
1.73	<i>Egln3</i>	EGL NINE HOMOLOG 3 (C. ELEGANS)
1.64	<i>Fadd</i>	FAS (TNFRSF6)-ASSOCIATED VIA DEATH DOMAIN
1.58	<i>Ntf3</i>	NEUROTROPHIN 3
Signaling molecules		
-1.53	<i>Cdc216</i>	CELL DIVISION CYCLE 2-LIKE 6 (CDK8-LIKE)
-1.69	<i>Cdc42se2</i>	CDC42 SMALL EFFECTOR 2
-1.73	<i>Csnk2a1</i>	CASEIN KINASE II, ALPHA 1 POLYPEPTIDE
-1.79	<i>Ddx1</i>	DEAD (ASP-GLU-ALA-ASP) BOX POLYPEPTIDE 1
-1.55	<i>Etnk1</i>	ETHANOLAMINE KINASE 1
-1.51	<i>Gnb2l1</i>	GUANINE NUCLEOTIDE BINDING PROTEIN (G PROTEIN), BETA POLYPEPTIDE 2 LIKE 1

-1.50	<i>Map3k7</i>	MITOGEN ACTIVATED PROTEIN KINASE KINASE KINASE 7
-1.69	<i>Mpp6</i>	MEMBRANE PROTEIN, PALMITOYLATED 6 (MAGUK P55 SUBFAMILY MEMBER 6)
-1.60	<i>Nme1</i>	EXPRESSED IN NON-METASTATIC CELLS 1, PROTEIN
-1.80	<i>Nme2</i>	EXPRESSED IN NON-METASTATIC CELLS 2, PROTEIN
-1.77	<i>Nme7</i>	NON-METASTATIC CELLS 7, PROTEIN EXPRESSED IN
-1.52	<i>Nt5c</i>	5',3'-NUCLEOTIDASE, CYTOSOLIC
-1.64	<i>Pank1</i>	PANTOTHENATE KINASE 1
-1.52	<i>Pdk1</i>	PYRUVATE DEHYDROGENASE KINASE, ISOENZYME 1
-1.62	<i>Pfkp</i>	PHOSPHOFRUCTOKINASE, PLATELET
-1.68	<i>Pgk1</i>	PHOSPHOGLYCERATE KINASE 1
-1.79	<i>Phpt1</i>	PHOSPHOHISTIDINE PHOSPHATASE 1
-1.74	<i>Pik3ca</i>	PHOSPHATIDYLINOSITOL 3-KINASE, CATALYTIC, ALPHA POLYPEPTIDE
-1.53	<i>Pip4k2a</i>	PHOSPHATIDYLINOSITOL-4-PHOSPHATE 5-KINASE, TYPE II, ALPHA
-1.62	<i>Ppp2r2a</i>	PROTEIN PHOSPHATASE 2 (FORMERLY 2A), REGULATORY SUBUNIT B (PR 52), ALPHA ISOFORM
-1.58	<i>Prps1</i>	PHOSPHORIBOSYL PYROPHOSPHATE SYNTHETASE 1
-1.70	<i>Prps2</i>	RIKEN CDNA 2610101M19 GENE
-1.53	<i>Pstk</i>	PHOSPHOSERYL-TRNA KINASE
-1.52	<i>Ptpn3</i>	PROTEIN TYROSINE PHOSPHATASE, NON-RECEPTOR TYPE 3
-1.86	<i>Ripk2</i>	RECEPTOR (TNFRSF)-INTERACTING SERINE-THREONINE KINASE 2
-1.61	<i>Rngt1</i>	RNA GUANYLYLTRANSFERASE AND 5'-PHOSPHATASE
-1.56	<i>Rock2</i>	RHO-ASSOCIATED COILED-COIL FORMING KINASE 2
-1.52	<i>Rps6ka3</i>	RIBOSOMAL PROTEIN S6 KINASE POLYPEPTIDE 3
-1.55	<i>Scy12</i>	SCY1-LIKE 2 (S. CEREVISIAE)
-1.51	<i>Smg7</i>	SMG-7 HOMOLOG, NONSENSE MEDIATED MRNA DECAY FACTOR (C. ELEGANS)
-1.51	<i>Srpk1</i>	SERINE/ARGININE-RICH PROTEIN SPECIFIC KINASE 1
-1.55	<i>Ssh2</i>	SLINGSHOT HOMOLOG 2 (DROSOPHILA)
-1.69	<i>Stk38</i>	RIKEN CDNA 5830476G13 GENE
-1.65	<i>Stk38l</i>	SERINE/THREONINE KINASE 38 LIKE
-1.72	<i>Styx</i>	PHOSPHOSERINE/THREONINE/TYROSINE INTERACTION PROTEIN
-1.81	<i>Traf3ip2</i>	TRAF3 INTERACTING PROTEIN 2
1.62	<i>Cish</i>	CYTOKINE INDUCIBLE SH2-CONTAINING PROTEIN
1.51	<i>Mst1r</i>	MACROPHAGE STIMULATING 1 RECEPTOR (C-MET-RELATED TYROSINE KINASE)
1.56	<i>Met</i>	MET PROTO-ONCOGENE
1.51	<i>Mapk6</i>	MITOGEN ACTIVATED PROTEIN KINASE 4
1.54	<i>Flrt2</i>	MITOGEN-ACTIVATED PROTEIN KINASE KINASE KINASE 5
1.67	<i>Pip5k1l</i>	PHOSPHATIDYLINOSITOL-4-PHOSPHATE 5-KINASE-LIKE 1
1.56	<i>Prkch</i>	PROTEIN KINASE C, ETA
1.62	<i>Pdk4</i>	PYRUVATE DEHYDROGENASE KINASE, ISOENZYME 4
1.68	<i>Mapk13</i>	SAPK/ERK/KINASE 4
1.69	<i>Snrk</i>	SNF RELATED KINASE

Data represent the average of 3 independent samples of WT and *Tcf7^{-/-}* memory OT-I T cells analyzed on Mouse GENE 1.0 ST arrays.

Negative fold changes indicate downregulated genes in *Tcf7^{-/-}* memory OT-I cells and are shown in bold.

Positive fold changes indicate upregulated genes in *Tcf7^{-/-}* memory OT-I cells. All fold changes are statistically significant, $p < 0.05$.

Each subset was listed on alphabetical order based on the gene symbols.

Genes highlighted in yellow are those among the top 20 upregulated or downregulated genes.